Research Article

Baboucarr Ceesay, Siegfried Macías, Muhammad Z. Baber, Nauman Ahmed, Alejandro Román-Loera, and Jorge E. Macías-Díaz*

Soliton-like solutions for a nonlinear doubly dispersive equation in an elastic Murnaghan's rod *via* Hirota's bilinear method

https://doi.org/10.1515/phys-2025-0189
received April 03, 2025; accepted June 30, 2025

Abstract: The purpose of this work is to study the physical phenomena of the doubly dispersive model that controls chaotic wave movement in the elastic Murnaghan's rod. The method of Hirota bilinear transformation is employed to derive various forms of solitary wave solutions, such as multiple waves, periodic lump waves, periodic cross-kink waves, homoclinic breather waves, dark soliton, and mixed waves. In order to see their physical behavior, we use the Mathematica software with selected values of the model parameters to depict their graphical behavior.

Keywords: doubly dispersive equation, Hirota bilinear transformation, periodic cross-kink, lump solutions, homoclinic breathers, multiwaves

*** Corresponding author: Jorge E. Macías-Díiaz,** Department of Mathematics, School of Digital Technologies, Tallinn University, Narva Rd. 25, 10120 Tallinn, Estonia; Departamento de Matemáticas y Fíisica, Universidad Autónoma de Aguascalientes, Avenida Universidad 940, Ciudad Universitaria, Aguascalientes 20131, Mexico, e-mail: jorge.macias_diaz@tlu.ee, jorge.maciasdiaz@edu.uaa.mx, tel: +52 449 910 8400; fax: +52 449 910 8401
Baboucarr Ceesay: Department of Mathematics and Statistics, The University of Lahore, Lahore, Pakistan; Mathematics Unit, The University of The Gambia, Serrekunda, Gambia, e-mail: bceesay@utg.edu.gm
Siegfried Macíias: Departamento de Matemáticas y Fíisica, Universidad Autónoma de Aguascalientes, Avenida Universidad 940, Ciudad Universitaria, Aguascalientes 20131, Mexico, e-mail: sigfrido.macias@edu.uaa.mx
Muhammad Z. Baber: Department of Mathematics and Statistics, The University of Lahore, Lahore, Pakistan, e-mail: zafarullah8883@gmail.com
Nauman Ahmed: Department of Mathematics and Statistics, The University of Lahore, Lahore, Pakistan, e-mail: nauman.ahmed@math.uol.edu.pk
Alejandro Román-Loera: Departamento de Sistemas Electrónicos, Universidad Autónoma de Aguascalientes, Avenida Universidad 940, Ciudad Universitaria, Aguascalientes 20131, Mexico, e-mail: alejandro.roman@edu.uaa.mx

1 Introduction

Nonlinear partial differential equations (NLPDEs) are used to characterize numerous physical phenomena that arise in real-world contexts [1,2]. They have many applications in scientific domains such as predator–prey systems with diffusion [3], fluid dynamics [4], plasma physics [5], nonlinear fiber optics [6], biological membrane [7], chaos theory for dynamical systems [8], ion acoustic [9], communication system [10], nonlinear elastic solids [11], and many other scientific disciplines. In that context, studies to derive traveling wave solutions and soliton solutions of NLPDE have been carried out by many investigators. That has led to the emergence of many techniques, such as the sine and cosine method [12], the simple equation method [13], the ϕ^6-expansion method [14], the Ricatti equation mapping method [15], Hirota's bilinear method [16], the Sardar sub-equation technique [17], the Jacobi elliptic function expansion (JEFE) method [18], the sinh-Gordon equation expansion method and its extended form [19,20], the $\frac{G'}{G^2}$-expansion technique [21], Darboux's transformation approach [22], the inverse scattering technique [23], the Bäcklund transformation approach [24], Piccard's iterative method [25], the homotopy analysis method [26], and many others.

The objective of this work is to employ the Hirota bilinear approach to obtain some novel exact traveling-wave solutions and soliton solutions for a doubly dispersive equation (DDE), which is obtained from nonlinear two-directional long-wave models for longitudinal waves in nonlinear dynamic elasticity. This model is expressed as [27]

$$Q_{tt} - \left(\frac{1}{\nu}(AQ)_x\right)_x - \frac{\delta}{2}\left(\frac{1}{\nu}(q\gamma Q^2 + \nu\lambda^2 Q_{tt} - (da\lambda^2 Q_x)_x)_x\right)_x = 0, \tag{1.1}$$

where $Q = Q(x,t)$ is the function of the wave strain, x is the spatial variable, t is the time, ν is the density, δ is a relatively small parameter, $q = \frac{B}{A}$ and $q = \frac{M}{A}$ represent the scale factors, and the Poisson parameter is given by

$a = \frac{A}{2(1+\lambda)}$. The DDE is a significant nonlinear evolution model commonly employed to describe wave motion in elastic media with spatial inhomogeneities, such as Murnaghan's rod [28]. This equation is significant in various engineering fields that deal with nonlinear elastic solids, especially in seismology, acoustics, and materials engineering. The solitary strain waves derived from the DDE have applications in long-distance power transmission, non-destructive testing (NDT) methods, and vibration paving of stiff materials.

The DDE has second-order time and space derivatives that are important in analyzing one-way or two-way traveling waves, such as shock waves, tsunamis, solitons, and wave structures. It is found to be of the same form as the Boussinesq equation in shallow water wave theory [29–32]. Solitons, which are derived from delayed differential equations, are significant in various fields. For example, they are used in seismology to describe the process of energy transfer in the course of earthquakes. In acoustics, they assist in the development of sound wave technologies. Soliton waves are also important in studying long-distance energy transfer without dissipation. Furthermore, solitary waves are essential for NDT, which is used to inspect materials such as pipelines and structural components without causing damage. The DDE also serves as a foundation for exploring nonlinear mechanics and condensed matter physics. The general form of the DDE after rescaling is (see [33])

$$Q_{tt} - k_1 Q_{xx} - (k_2 Q^2 + k_3 Q_{tt} + k_4 Q_{xx})_{xx} = 0. \tag{1.2}$$

This equation encompasses the appropriate balance between the second time and spatial derivatives with the help of both nonlinear and dispersive constituents. The symbols k_1, k_2, k_3, and k_4 are non-dimensional parameters, which are specific to the material and influence wave propagation in the medium.

There are many reports in the literature that study DDE solutions. For example, using the sine-Gordon expansion technique, Yel [34] obtained traveling-wave solutions of the DDE in nonlinear dynamic elasticity. On the other hand, Cattani *et al.* [27] adapted the extended sinh-Gordon expansion approach and the modified $\exp(-\phi(\xi))$ expansion approach to obtain singular topological and non-topological soliton-type and periodic wave solutions for the DDE. Ahmed *et al.* [35] implemented the improved modified extended tanh-function technique on the DDE and generated novel solutions, such as bright and dark solitons, Jacobi elliptic solutions and Weiss elliptic solutions. Alharthi [36] considered DDE in order to explain the phenomena of wave propagation utilizing the extended generalized exponential rational function technique and the Jacobi elliptic function technique on the contour sets, thus obtaining new solutions. Meanwhile, Rehman *et al.* [37] used the Sardar sub-equation method (SSEM) to find various wave solutions to the DDE for Murnaghan's rod. Some works by Ozisik *et al.* [38] were devoted to investigating the extended Kudryashov technique together with the Bernoulli–Riccati technique to find the solution of the DDE. In that way, they reached topological, non-topological and singular solitons, periodic, and rational solutions.

On the other hand, Ibrahim *et al.* [39] derived optical solitons of the DDE *via* the Sardar sub-equation. Those solutions describe shallow water flow in a vertically vibrating container with a free surface of small depth. Younas *et al.* [40] studied the DDE in Murnaghan's rod and derived several soliton solutions through the new extended direct algebraic method new extended direct algebraic method and the generalized Kudryashov method GKM. The DDE for Murnaghan's rod was solved by Silambarasan *et al.* [30] using the F-expansion method. They obtained periodic wave solutions as well as non-topological, singular, and compound solitons. Abourabia and Eldreeny [41] addressed the DDE for strain waves in cylindrical rods by using the ecommutative hyper-complex algebraic method. Their results exhibited the characteristics of solitary waves and their stability was analyzed by using phase portraits. Also, Asjad *et al.* [42] gave new solutions in the form of traveling waves for the DDE *via* the direct algebraic extended method. In such way, they produced a number of different types of solutions. Dusunceli *et al.* [43] applied the improved Bernoulli sub-equation function method (IBSEFM) to the solution of the DDE and calculated some traveling-wave solutions.

It is worth pointing out that Alquran and Al-Smadi [33] presented various bidirectional wave solutions to the generalized DDE using the modified rational sine-cosine and sinh-cosh functions in conjunction with the unified method. In this context, Eremeyev and Kolpakov [44] adopted a numerical approach to investigate the wave propagation in elastic inhomogeneous materials. These authors reported on the solitary wave regime and the analysis of its properties. Eremeyev *et al.* [45] also used the same model to examine harmonic wave propagation in elastic inhomogeneous materials with rheology. In this case, the authors were able to compute analytical solutions to the dispersion relations and wave travel for different materials. In turn, Islam [46] used the modified Khater approach to investigate some wave solutions to the DDE. By examining the system's dynamics, stability, and bifurcation, this author offered novel analytical perspectives. Khatun *et al.* [47] investigated the beta space–time fractional DDE employing the $(\frac{G'}{G}, \frac{1}{G})$-expansion method to derive different exact soliton solutions, such as circular, hyperbolic, and rational forms. They also investigated stability

via linear analysis and bifurcation theory to uncover varied wave structures applicable in nonlinear elasticity, plasma, acoustics, and seismic research. Khater *et al.* [48] examined the (2 + 1)-dimensional Zabolotskaya–Khokhlov equation with dissipation by employing the Khater II method, modified Kudryashov method, and He's variational iteration scheme. The exact and numerical solutions are derived, indicating exact complex dispersive and dissipative wave structures. The obtained results supply valuable information for acoustics, fluid mechanics, and nonlinear optics. Naz *et al.* [49] appllied the modified exponential method to the fractional-order longitudinal wave equation of a magneto-elastic circular rod with conformable derivative theory. New kink-shaped, bell-shaped, and bright soliton solutions are given in the study, which are of significant physical interest from the graphical analysis. The results are of paramount significance to tsunami modeling, wave dynamics, and fractional-order magneto-elastic systems. However, out of all of the analytical approaches mentioned so far, the Hirota bilinear method is perhaps one of the most valuable tools in soliton research. It has greatly contributed to the understanding of complicated wave structures generated by diverse NLPDEs.

As we will point out in the following section, the extensive applicability of the Hirota bilinear method has been thoroughly demonstrated in the literature. The results obtained through this method go beyond the derivation of classical solitons and includes various other interesting wave shapes, such as rogue, singular, kink, anti-kink, breather, M-shaped, and lump waves. Such solutions are not merely theoretical in nature and can be found in practical usage, as in wave optical pulses, biological membranes, fluids dynamics, modeling of shallow water waves, etc. In summary, these reports exhibit the relevance of the Hirota bilinear method across disciplines, especially in improving our understanding of waves and soliton solutions and their applications in real life. In this work, we will employ the Hirota bilinear transformation method to derive solutions of the DDE described in Eq. (1.2). We have thoroughly reviewed the specialized literature, and, to the best of our knowledge, the Hirota bilinear transformation approach has not yet been applied to the DDE in previous studies. Moreover, wave solutions have not been obtained through this method, and effects of the model parameters were not addressed either. This points out a gap in the research literature which this study seeks to address.

2 Method

It is important to note that various researchers have employed the Hirota bilinear method in recent years to obtain exact solutions to a variety of NLPDEs. For example, Alsallami *et al.* [50] were able to solve the stochastic fractional Drinfel'd–Sokolov–Wilson equation, Garcia Guirao *et al.* [51] used the method to study the fourth-order extended (2 + 1)-dimensional Boussinesq equation, and Ceesay *et al.* [52] were able to study the fluid ionic wave phenomena. In turn, Yang and Wei [53] also utilized Hirota's bilinear technique to derive bilinear equations with indeterminate coefficients for NLPDEs. In a similar setting, Wazwaz [54] applied both the tanh–coth and Hirota's bilinear method, and was able to obtain numerous solutions to the problem of Sawada–Kotera–Kadmotsev–Petviashvili. An extensive work on bilinear method was performed by Hereman and Zhuang [55]. Moreover, other investigators have also used the Hirota bilinear method in their research on different models. For instance, Rizvi *et al.* [56] employed the Hirota bilinear method to study saturated ferromagnets. Wang *et al.* [57] conducted research of plasma and fluid dynamics for the generalized (3 + 1)-dimensional Kadomtsev–Petviashvili model, while Khan and Wazwaz [58] also used this method with *ansatz* functions to derive several new shapes and many-breather solutions. In addition, Zhao *et al.* [59] studied the asymmetric (2 + 1)-Nizhnik–Novikov–Veselov model to provide some lump and mixed lump-stripe wave solutions. By employing this approach, Ren *et al.* [60] explored the Calogero–Bogoyavlenskii–Schiff system in dimensions. Also, Rizvi *et al.* [61] investigated the coupled Higgs equations *via* this technique and Yel *et al.* [62] studied the Hirota–Maccari system.

In the following, we will derive solutions of the DDE using the Hirota bilinear method. More precisely, we solve Eq. (1.2) under the assumption that there exist solutions satisfying

$$\begin{aligned} Q(x,t) &= P(\varrho), \\ \varrho &= x - \beta t. \end{aligned} \tag{2.1}$$

In this transformation, the parameter $\beta \neq 0$ represents the wave velocity. Using this transformation, the NLPDE becomes an ordinary differential equation (ODE) *via* the function P of ϱ. Eq. (2.1) is used then to transform Eq. (1.2) into the ODE:

$$-k_2P^2 + (-(\beta^2k_3 + k_4))\frac{\mathrm{d}^2P}{\mathrm{d}\varrho^2} + P(\beta^2 - k_1) = 0. \tag{2.2}$$

We use Eq. (2.2) to determine the different wave structures that arise from (1.2).

First, suppose that the solution of Eq. (2.2) is of the form

$$P(\varrho) = \frac{m\left(\Omega\frac{\mathrm{d}^2\Omega}{\mathrm{d}\varrho^2} - \left(\frac{\mathrm{d}\Omega}{\mathrm{d}\varrho}\right)^2\right)}{\Omega^2}, \tag{2.3}$$

where $\Omega = \Omega(\varrho)$ represents the class of wave functions considered, and $m \neq 0$ is a constant to be determined. Upon substituting Eq. (2.3) into Eq. (2.2), we obtain

$$
\begin{aligned}
0 = \Omega^3\Bigg[&(\beta^2 k_3 + k_4)\frac{\mathrm{d}^4\Omega}{\mathrm{d}\varrho^4} + (k_1 - \beta^2)\frac{\mathrm{d}^2\Omega}{\mathrm{d}\varrho^2}\Bigg] \\
&+ (k_2 m - 6(\beta^2 k_3 + k_4))\left(\frac{\mathrm{d}\Omega}{\mathrm{d}\varrho}\right)^4 \\
&+ 2\Omega(6(\beta^2 k_3 + k_4) - k_2 m)\frac{\mathrm{d}^2\Omega}{\mathrm{d}\varrho^2}\left(\frac{\mathrm{d}\Omega}{\mathrm{d}\varrho}\right)^2 \\
&+ \Omega^2\Bigg[(\beta^2 - k_1)\left(\frac{\mathrm{d}\Omega}{\mathrm{d}\varrho}\right)^2 - 4(\beta^2 k_3 + k_4)\frac{\mathrm{d}^3\Omega}{\mathrm{d}\varrho^3}\frac{\mathrm{d}\Omega}{\mathrm{d}\varrho} \\
&+ (k_2 m - 3(\beta^2 k_3 + k_4))\left(\frac{\mathrm{d}^2\Omega}{\mathrm{d}\varrho^2}\right)^2\Bigg].
\end{aligned} \tag{2.4}
$$

3 Results

We derive various wave structures in the sequel from Eq. (2.4). To that end, we consider various forms of the function $\Omega(\varrho)$. For brevity, if P_* represents a solution of (2.3), then the corresponding solution of the DDE will be denoted by $Q_*(x, t) = P_*(\varrho) = P_*(x - \beta t)$.

3.1 Multi-wave solutions

Following the approach used in previous studies [63,64], we will derive multi-wave solutions by using the function

$$
\begin{aligned}
\Omega(\varrho) = {} & h_1 \cosh(z(g_1\varrho + g_2)) + h_2 \cos(z(g_3\varrho + g_4)) \\
& + h_3 \cosh(z(g_5\varrho + g_6)),
\end{aligned} \tag{3.1}
$$

where g_i, h_j, and $z \neq 0$ are the arbitrary constants, for each $1 \leq i \leq 6$ and $1 \leq j \leq 3$. We substitute Eq. (3.1) into (2.4). Next, set the hyperbolic and trigonometric function coefficients equal to zero. After reducing algebraically, we obtain the following two groups of solutions:

Group 1

In this case, we consider the constants

$$
\begin{aligned}
g_1 &= \frac{\sqrt{\beta^2 - k_1}}{\sqrt{4\beta^2 k_3 z^2 + 4k_4 z^2}}, \quad g_3 = \frac{\sqrt{k_1 - \beta^2}}{2\sqrt{\beta^2 k_3 z^2 + k_4 z^2}}, \\
g_5 &= \frac{\sqrt{\beta^2 - k_1}}{\sqrt{4\beta^2 k_3 z^2 + 4k_4 z^2}}, \quad m = \frac{6(\beta^2 k_3 + k_4)}{k_2},
\end{aligned} \tag{3.2}
$$

where $k_1, k_2, k_3, k_4 \neq 0$ are the free constant parameters. We substitute these constants into Eq. (3.1). Next, we employ the result in Eq. (2.3) to obtain the solution

$$
P_{1MU}(\varrho) = -\frac{3\left(\frac{\left(A_1\sqrt{\beta^2 - k_1} - h_2\sqrt{k_1 - \beta^2}\sin\left(z\left(g_4 + \frac{\varrho\sqrt{k_1 - \beta^2}}{2\sqrt{z^2(\beta^2 k_3 + k_4)}}\right)\right)\right)^2}{\left(A_2 + h_3\cosh\left(z\left(g_6 + \frac{\varrho\sqrt{\beta^2 - k_1}}{2\sqrt{z^2(\beta^2 k_3 + k_4)}}\right)\right)\right)^2} - \beta^2 + k_1\right)}{2k_2}, \tag{3.3}
$$

where

$$
\begin{aligned}
A_1 = {} & h_1 \sinh\left(z\left(g_2 + \frac{\varrho\sqrt{\beta^2 - k_1}}{2\sqrt{z^2(\beta^2 k_3 + k_4)}}\right)\right) \\
& + h_3 \sinh\left(z\left(g_6 + \frac{\varrho\sqrt{\beta^2 - k_1}}{2\sqrt{z^2(\beta^2 k_3 + k_4)}}\right)\right),
\end{aligned} \tag{3.4}
$$

$$
\begin{aligned}
A_2 = {} & h_2 \cos\left(z\left(g_4 + \frac{\varrho\sqrt{k_1 - \beta^2}}{2\sqrt{z^2(\beta^2 k_3 + k_4)}}\right)\right) \\
& + h_1 \cosh\left(z\left(g_2 + \frac{\varrho\sqrt{\beta^2 - k_1}}{2\sqrt{z^2(\beta^2 k_3 + k_4)}}\right)\right).
\end{aligned} \tag{3.5}
$$

Group 2

In this case, we will consider the constant $h_1 = 0$, along with

$$
\begin{aligned}
g_3 &= -\frac{\sqrt{k_1 - \beta^2}}{2\sqrt{\beta^2 k_3 z^2 + k_4 z^2}}, \\
g_5 &= -\frac{\sqrt{\beta^2 - k_1}}{\sqrt{4\beta^2 k_3 z^2 + 4k_4 z^2}}, \\
m &= \frac{6(\beta^2 k_3 + k_4)}{k_2},
\end{aligned} \tag{3.6}
$$

where $k_1, k_2, k_3, k_4 \neq 0$ are the free parameters. Using these constants in Eq. (3.1), substituting the result then into Eq. (2.3), we readily reach that

$$
P_{2MU}(\varrho) = \frac{A_5 + 6h_2h_3(\beta^2 - k_1)\cos\left(z\left(g_4 - \frac{\varrho\sqrt{k_1 - \beta^2}}{2\sqrt{z^2(\beta^2 k_3 + k_4)}}\right)\right)\cosh\left(z\left(g_6 - \frac{\varrho\sqrt{\beta^2 - k_1}}{2\sqrt{z^2(\beta^2 k_3 + k_4)}}\right)\right)}{2k_2\left(h_2\cos\left(z\left(g_4 - \frac{\varrho\sqrt{k_1 - \beta^2}}{2\sqrt{z^2(\beta^2 k_3 + k_4)}}\right)\right) + h_3\cosh\left(z\left(g_6 - \frac{\varrho\sqrt{\beta^2 - k_1}}{2\sqrt{z^2(\beta^2 k_3 + k_4)}}\right)\right)\right)^2}, \tag{3.7}
$$

where

$$A_5 = 6h_3h_2\sqrt{-(\beta^2 - k_1)^2}\,\sin\left(z\left(g_4 - \frac{\varrho\sqrt{k_1 - \beta^2}}{2\sqrt{z^2(\beta^2k_3 + k_4)}}\right)\right) \times \sinh\left(z\left(g_6 - \frac{\varrho\sqrt{\beta^2 - k_1}}{2\sqrt{z^2(\beta^2k_3 + k_4)}}\right)\right) + 3h_2^2(\beta^2 - k_1) + 3h_3^2(\beta^2 - k_1). \tag{3.8}$$

3.2 Periodic lump solutions

In this case, we follow the approach used in [63,64], and allow

$$\Omega(\varrho) = (g_1\varrho + g_2)^2 + (g_3\varrho + g_4)^2 + \cos(g_5\varrho + g_6) + g_7, \tag{3.9}$$

where g_i, for each $1 \le i \le 7$, are the arbitrary constants. We substitute Eq. (3.9) into Eq. (2.4). Next, we set ϱ and the trigonometric function coefficients equal to zero. In that way, we obtain solutions for the constant parameter values $g_1 = -ig_3$, $g_2 = -ig_4$, $g_7 = 0$, and

$$g_5 = -\frac{\sqrt{k_1 - \beta^2}}{2\sqrt{\beta^2k_3 + k_4}}, \quad m = \frac{6(\beta^2k_3 + k_4)}{k_2}, \tag{3.10}$$

where $k_1, k_2, k_3, k_4 \neq 0$ are the free parameters. Substituting these values into Eqs. (3.9) and (2.3), we obtain that

$$P_{1PL}(\varrho) = \frac{3(\beta^2 - k_1)\sec^2\left(g_6 - \frac{\varrho\sqrt{k_1 - \beta^2}}{2\sqrt{\beta^2k_3 + k_4}}\right)}{2k_2}. \tag{3.11}$$

3.3 Periodic cross-kink solutions

In order to derive periodic cross-kink solutions of the DDE, we follow [65,66] and define

$$\Omega(\varrho) = h_1\exp(z(g_3\varrho + g_4)) + \exp(-z(g_1\varrho + g_2)) + h_2\cos(z(g_5\varrho + g_6)) + h_3\cosh(z(g_7\varrho + g_8)) + g_9, \tag{3.12}$$

where g_i, h_j, and $z \neq 0$ are the arbitrary constants, for each $1 \le i \le 9$ and $1 \le j \le 3$. We substitute Eq. (3.12) into Eq. (2.4). Next, we set the exponential, hyperbolic, and trigonometric function coefficients equal to zero, to obtain the following groups of solutions.

Group 1

We set $h_2 = 0$, $g_9 = 0$, and

$$g_1 = -\frac{\sqrt{\beta^2 - k_1}}{2\sqrt{z^2(\beta^2k_3 + k_4)}}, \quad g_3 = -\frac{\sqrt{\beta^2 - k_1}}{2\sqrt{z^2(\beta^2k_3 + k_4)}}, \quad g_7 = \frac{\sqrt{\beta^2 - k_1}}{2\sqrt{z^2(\beta^2k_3 + k_4)}}, \quad m = \frac{6(\beta^2k_3 + k_4)}{k_2}, \tag{3.13}$$

where $k_1, k_2, k_3, k_4 \neq 0$ are the free parameters. After replacing these values into Eq. (3.12), and then into Eq. (2.3), we reach the solution

$$P_{1PCK}(\varrho) = \frac{3(\beta^2 - k_1)(2h_1e^{(g_4+g_8)z} + h_3)(h_3e^{(g_2+g_8)z} + 2)\exp\left(-z\left(-g_2 + g_8 + \frac{\varrho\sqrt{\beta^2 - k_1}}{\sqrt{z^2(\beta^2k_3 + k_4)}}\right)\right)}{2k_2\left(A_7 + h_1\exp\left(z\left(g_2 + g_4 - \frac{\varrho\sqrt{\beta^2 - k_1}}{\sqrt{z^2(\beta^2k_3 + k_4)}}\right)\right) + 1\right)^2}, \tag{3.14}$$

where

$$A_7 = h_3\exp\left(z\left(g_2 - \frac{\varrho\sqrt{\beta^2 - k_1}}{2\sqrt{z^2(\beta^2k_3 + k_4)}}\right)\right) \times \cosh\left(z\left(g_8 + \frac{\varrho\sqrt{\beta^2 - k_1}}{2\sqrt{z^2(\beta^2k_3 + k_4)}}\right)\right). \tag{3.15}$$

Group 2

In this case, we let $h_1 = 0$, $g_9 = 0$, and

$$g_1 = -\frac{\sqrt{\beta^2 - k_1}}{2\sqrt{z^2(\beta^2 k_3 + k_4)}}, \quad g_5 = -\frac{\sqrt{k_1 - \beta^2}}{2\sqrt{z^2(\beta^2 k_3 + k_4)}}, \quad g_7 = -\frac{\sqrt{\beta^2 - k_1}}{2\sqrt{z^2(\beta^2 k_3 + k_4)}}, \quad m = \frac{6(\beta^2 k_3 + k_4)}{k_2}, \tag{3.16}$$

where $k_1, k_2, k_3, k_4 \neq 0$ are the free parameters. Substituting these values into Eq. (3.12), and then the result into Eq. (2.3), yields the following solution:

$$P_{2PCK}(\varrho) = \frac{3\left((A_9 + 1)^2(\beta^2 - k_1)\exp\left(\frac{z\varrho\sqrt{\beta^2 - k_1}}{\sqrt{z^2(\beta^2 k_3 + k_4)}} - 2g_2 z\right) - A_{10}^2\right)}{2k_2\left(A_{11} + \exp\left(-z\left(g_2 - \frac{\varrho\sqrt{\beta^2 - k_1}}{2\sqrt{z^2(\beta^2 k_3 + k_4)}}\right)\right)\right)^2}. \tag{3.17}$$

Here,

$$A_9 = \exp\left(z\left(g_2 - \frac{\varrho\sqrt{\beta^2 - k_1}}{2\sqrt{z^2(\beta^2 k_3 + k_4)}}\right)\right) \times \left(h_2 \cos\left(z\left(g_6 - \frac{\varrho\sqrt{k_1 - \beta^2}}{2\sqrt{z^2(\beta^2 k_3 + k_4)}}\right)\right) + h_3 \cosh\left(z\left(g_8 - \frac{\varrho\sqrt{\beta^2 - k_1}}{2\sqrt{z^2(\beta^2 k_3 + k_4)}}\right)\right)\right), \tag{3.18}$$

$$A_{10} = \sqrt{\beta^2 - k_1}\left(\exp\left(-z\left(g_2 - \frac{\varrho\sqrt{\beta^2 - k_1}}{2\sqrt{z^2(\beta^2 k_3 + k_4)}}\right)\right) - h_3 \sinh\left(z\left(g_8 - \frac{\varrho\sqrt{\beta^2 - k_1}}{2\sqrt{z^2(\beta^2 k_3 + k_4)}}\right)\right)\right) + h_2\sqrt{k_1 - \beta^2}\sin\left(z\left(g_6 - \frac{\varrho\sqrt{k_1 - \beta^2}}{2\sqrt{z^2(\beta^2 k_3 + k_4)}}\right)\right) \tag{3.19}$$

and

$$A_{11} = h_2 \cos\left(z\left(g_6 - \frac{\varrho\sqrt{k_1 - \beta^2}}{2\sqrt{z^2(\beta^2 k_3 + k_4)}}\right)\right) + h_3 \cosh\left(z\left(g_8 - \frac{\varrho\sqrt{\beta^2 - k_1}}{2\sqrt{z^2(\beta^2 k_3 + k_4)}}\right)\right). \tag{3.20}$$

3.4 Homoclinic breather solutions

Following previous studies [65,66], homoclinic breather solutions are obtained when

$$\Omega(\varrho) = h_1 \exp(z(g_3\varrho + g_4)) + \exp(-z(g_1\varrho + g_2)) + h_2 \cos(z(g_5\varrho + g_6)), \tag{3.21}$$

where g_i, h_j, and $z \neq 0$ are the arbitrary constants, for each $1 \leq i \leq 6$ and $1 \leq j \leq 2$. Proceeding as before, we substitute Eq. (3.12) into Eq. (2.4). Next, we set the exponential and trigonometric function coefficients equal to zero, in order to derive two groups of solutions.

Group 1

In this case, we let

$$g_1 = \frac{\sqrt{\beta^2 - k_1}}{\sqrt{4\beta^2 k_3 z^2 + 4k_4 z^2}}, \quad g_3 = \frac{\sqrt{\beta^2 - k_1}}{2\sqrt{z^2(\beta^2 k_3 + k_4)}}, \quad g_5 = -\frac{\sqrt{k_1 - \beta^2}}{2\sqrt{\beta^2 k_3 z^2 + k_4 z^2}}, \quad m = \frac{6(\beta^2 k_3 + k_4)}{k_2}, \tag{3.22}$$

where $k_1, k_2, k_3, k_4 \neq 0$ are the free constant parameters. Inserting these values into Eq. (3.21), and then the result into Eq. (2.3), we reach the solution

$$P_{1HB}(\varrho) = \frac{3(A_{16}\sqrt{-(\beta^2 - k_1)^2} + A_{15}(\beta^2 - k_1))\exp\left(z\left(g_2 + \frac{\varrho\sqrt{\beta^2 - k_1}}{2\sqrt{z^2(\beta^2 k_3 + k_4)}}\right)\right)}{2k_2\left(A_{17} + h_1 \exp\left(z\left(g_2 + g_4 + \frac{\varrho\sqrt{\beta^2 - k_1}}{\sqrt{z^2(\beta^2 k_3 + k_4)}}\right)\right) + 1\right)^2}, \tag{3.23}$$

where

$$A_{15} = \left(h_2^2 \exp\left(z\left(g_2 + \frac{\varrho\sqrt{\beta^2 - k_1}}{2\sqrt{z^2(\beta^2 k_3 + k_4)}}\right)\right) + 4h_1 \exp\left(z\left(g_4 + \frac{\varrho\sqrt{\beta^2 - k_1}}{2\sqrt{z^2(\beta^2 k_3 + k_4)}}\right)\right)\right) + 2h_2 \cos\left(z\left(g_6 - \frac{\varrho\sqrt{k_1 - \beta^2}}{2\sqrt{z^2(\beta^2 k_3 + k_4)}}\right)\right) \times \left(h_1 \exp\left(z\left(g_2 + g_4 + \frac{\varrho\sqrt{\beta^2 - k_1}}{\sqrt{z^2(\beta^2 k_3 + k_4)}}\right)\right) + 1\right), \tag{3.24}$$

$$A_{16} = -2h_1h_2 \exp\left(z\left(g_2 + g_4 + \frac{\varrho\sqrt{\beta^2 - k_1}}{\sqrt{z^2(\beta^2k_3 + k_4)}}\right)\right) \times \sin\left(z\left(g_6 - \frac{\varrho\sqrt{k_1 - \beta^2}}{2\sqrt{z^2(\beta^2k_3 + k_4)}}\right)\right) + 2h_2 \sin\left(z\left(g_6 - \frac{\varrho\sqrt{k_1 - \beta^2}}{2\sqrt{z^2(\beta^2k_3 + k_4)}}\right)\right), \tag{3.25}$$

and

$$A_{17} = h_2 \exp\left(z\left(g_2 + \frac{\varrho\sqrt{\beta^2 - k_1}}{2\sqrt{z^2(\beta^2k_3 + k_4)}}\right)\right) \times \cos\left(z\left(g_6 - \frac{\varrho\sqrt{k_1 - \beta^2}}{2\sqrt{z^2(\beta^2k_3 + k_4)}}\right)\right). \tag{3.26}$$

Group 2

In this group, we let $h_1 = 0$,

$$g_1 = \frac{\sqrt{\beta^2 - k_1}}{\sqrt{4\beta^2k_3z^2 + 4k_4z^2}}, \quad g_5 = -\frac{\sqrt{k_1 - \beta^2}}{2\sqrt{\beta^2k_3z^2 + k_4z^2}}, \quad m = \frac{6(\beta^2k_3 + k_4)}{k_2}, \tag{3.27}$$

where $k_1, k_2, k_3, k_4 \neq 0$ are the free constant parameters. Proceeding as in the other cases, we obtain the solution

$$P_{2HB}(\varrho)\frac{3h_2 \exp\left(z\left(g_2 + \frac{\varrho\sqrt{\beta^2 - k_1}}{2\sqrt{z^2(\beta^2k_3 + k_4)}}\right)\right)\left(A_{21} + 2(\beta^2 - k_1)\cos\left(z\left(g_6 - \frac{\varrho\sqrt{k_1 - \beta^2}}{2\sqrt{z^2(\beta^2k_3 + k_4)}}\right)\right)\right)}{2k_2\left(h_2 \exp\left(z\left(g_2 + \frac{\varrho\sqrt{\beta^2 - k_1}}{2\sqrt{z^2(\beta^2k_3 + k_4)}}\right)\right)\cos\left(z\left(g_6 - \frac{\varrho\sqrt{k_1 - \beta^2}}{2\sqrt{z^2(\beta^2k_3 + k_4)}}\right)\right) + 1\right)^2}, \tag{3.28}$$

where

$$A_{21} = h_2(\beta^2 - k_1)\exp\left(z\left(g_2 + \frac{\varrho\sqrt{\beta^2 - k_1}}{2\sqrt{z^2(\beta^2k_3 + k_4)}}\right)\right) + 2\sqrt{-(\beta^2 - k_1)^2}\sin\left(z\left(g_6 - \frac{\varrho\sqrt{k_1 - \beta^2}}{2\sqrt{z^2(\beta^2k_3 + k_4)}}\right)\right). \tag{3.29}$$

3.5 Interaction of two-exponent solution

In this case, we follow previous studies [66,67] to obtain solutions with the interaction of two exponents. To that end, we let

$$\Omega(\varrho) = h_1 \exp(z(g_3\varrho + g_4)) + h_2 \exp(z(g_1\varrho + g_2)), \tag{3.30}$$

where g_i, h_j, and $z \neq 0$ are the arbitrary constants, for each $1 \leq i \leq 4$ and $1 \leq j \leq 2$. Proceeding as earlier, we substitute Eq. (3.30) into Eq. (2.4). We set the exponential function coefficients equal to zero. In this case, we obtain tone group of solutions by letting

$$g_1 = g_3 + \frac{k_1 - \beta^2}{\sqrt{z^2(\beta^2 - k_1)(\beta^2k_3 + k_4)}}, \quad m = \frac{6(\beta^2k_3 + k_4)}{k_2}, \tag{3.31}$$

where $k_1, k_2, k_3, k_4 \neq 0$ are the free parameters. Substitute these constants into Eq. (3.30), and then the result into Eq. (2.3) to reach the solution

$$P_{1MI}(\varrho) = \frac{6h_1h_2(\beta^2 - k_1)\exp\left(z\left(2g_3\varrho + g_2 + g_4 + \frac{\varrho(k_1 - \beta^2)}{\sqrt{z^2(\beta^2 - k_1)(\beta^2k_3 + k_4)}}\right)\right)}{k_2\left(h_2 \exp\left(z\left(\varrho\left(g_3 + \frac{k_1 - \beta^2}{\sqrt{z^2(\beta^2 - k_1)(\beta^2k_3 + k_4)}}\right) + g_2\right)\right) + h_1e^{z(g_3\varrho + g_4)}\right)^2}. \tag{3.32}$$

3.6 Mixed wave solutions

This type of wave structure function is offered by letting [66,67]

$$\Omega(\varrho) = h_1 \exp(z(g_1\varrho + g_2)) + h_2 \exp(-z(g_1\varrho + g_2)) + h_3 \sin(z(g_3\varrho + g_4)) + h_4 \sinh(z(g_5\varrho + g_6)), \tag{3.33}$$

where g_i, h_j, and $z \neq 0$ are the arbitrary constants, for each $1 \leq i \leq 6$ and $1 \leq j \leq 4$. We substitute Eq. (3.33) into Eq. (2.4), and set the exponential, hyperbolic, and trigonometric function coefficients equal to zero. Two groups of solutions are derived in this case.

Group 1

In this group, we let

$$g_1 = \frac{\sqrt{\beta^2 - k_1}}{\sqrt{4\beta^2 k_3 z^2 + 4k_4 z^2}}, \quad g_3 = -\frac{\sqrt{k_1 - \beta^2}}{2\sqrt{\beta^2 k_3 z^2 + k_4 z^2}}, \quad g_5 = -\frac{\sqrt{\beta^2 - k_1}}{\sqrt{4\beta^2 k_3 z^2 + 4k_4 z^2}}, \quad m = \frac{6(\beta^2 k_3 + k_4)}{k_2}, \tag{3.34}$$

where $k_1, k_2, k_3, k_4 \neq 0$ are the free parameters. Substituting these values into Eq. (3.33) and into Eq. (2.3), we have

$$P_{1MI}(\varrho) = \frac{3(A_{23}^2(\beta^2 - k_1) - A_{24}^2)\exp\left(-2z\left(g_2 + \frac{\varrho\sqrt{\beta^2 - k_1}}{2\sqrt{z^2(\beta^2 k_3 + k_4)}}\right)\right)}{2k_2\left(A_{25} + h_1\exp\left(z\left(g_2 + \frac{\varrho\sqrt{\beta^2 - k_1}}{2\sqrt{z^2(\beta^2 k_3 + k_4)}}\right)\right)\right)^2}, \tag{3.35}$$

where

$$\begin{aligned} A_{23} = {} & h_1\exp\left(2g_2 z + \frac{z\varrho\sqrt{\beta^2 - k_1}}{\sqrt{z^2(\beta^2 k_3 + k_4)}}\right) \\ & + \exp\left(z\left(g_2 + \frac{\varrho\sqrt{\beta^2 - k_1}}{2\sqrt{z^2(\beta^2 k_3 + k_4)}}\right)\right) \\ & \cdot\left(h_3\sin\left(z\left(g_4 - \frac{\varrho\sqrt{k_1 - \beta^2}}{2\sqrt{z^2(\beta^2 k_3 + k_4)}}\right)\right)\right. \\ & \left. + h_4\sinh\left(z\left(g_6 - \frac{\varrho\sqrt{\beta^2 - k_1}}{2\sqrt{z^2(\beta^2 k_3 + k_4)}}\right)\right)\right) + h_2, \end{aligned} \tag{3.36}$$

$$\begin{aligned} A_{24} = {} & h_2\sqrt{\beta^2 - k_1} - h_1\sqrt{\beta^2 - k_1} \\ & \times\exp\left(2g_2 z + \frac{z\varrho\sqrt{\beta^2 - k_1}}{\sqrt{z^2(\beta^2 k_3 + k_4)}}\right) \\ & + \exp\left(z\left(g_2 + \frac{\varrho\sqrt{\beta^2 - k_1}}{2\sqrt{z^2(\beta^2 k_3 + k_4)}}\right)\right) \\ & \cdot\left(h_3\sqrt{k_1 - \beta^2}\cos\left(z\left(g_4 - \frac{\varrho\sqrt{k_1 - \beta^2}}{2\sqrt{z^2(\beta^2 k_3 + k_4)}}\right)\right)\right. \\ & \left. + h_4\sqrt{\beta^2 - k_1}\cosh\left(z\left(g_6 - \frac{\varrho\sqrt{\beta^2 - k_1}}{2\sqrt{z^2(\beta^2 k_3 + k_4)}}\right)\right)\right), \end{aligned} \tag{3.37}$$

and

$$\begin{aligned} A_{25} = {} & h_2\exp\left(-z\left(g_2 + \frac{\varrho\sqrt{\beta^2 - k_1}}{2\sqrt{z^2(\beta^2 k_3 + k_4)}}\right)\right) \\ & + h_3\sin\left(z\left(g_4 - \frac{\varrho\sqrt{k_1 - \beta^2}}{2\sqrt{z^2(\beta^2 k_3 + k_4)}}\right)\right) \\ & + h_4\sinh\left(z\left(g_6 - \frac{\varrho\sqrt{\beta^2 - k_1}}{2\sqrt{z^2(\beta^2 k_3 + k_4)}}\right)\right). \end{aligned} \tag{3.38}$$

Group 2

Let now $h_2 = 0$,

$$g_1 = \frac{\sqrt{\beta^2 - k_1}}{2\sqrt{z^2(\beta^2 k_3 + k_4)}}, \quad g_3 = -\frac{\sqrt{k_1 - \beta^2}}{2\sqrt{z^2(\beta^2 k_3 + k_4)}}, \quad g_5 = \frac{\sqrt{\beta^2 - k_1}}{2\sqrt{z^2(\beta^2 k_3 + k_4)}}, \quad m = \frac{6(\beta^2 k_3 + k_4)}{k_2}, \tag{3.39}$$

where $k_1, k_2, k_3, k_4 \neq 0$ are the free constants. Proceeding as before, we reach the solution

$$P_{2MI}(\varrho) = -\frac{3\left(\frac{\left(A_{29}\sqrt{\beta^2 - k_1} - h_3\sqrt{k_1 - \beta^2}\cos\left(z\left(g_4 - \frac{\varrho\sqrt{k_1 - \beta^2}}{2\sqrt{z^2(\beta^2 k_3 + k_4)}}\right)\right)\right)^2}{\left(A_{30} + h_1\exp\left(z\left(g_2 + \frac{\varrho\sqrt{\beta^2 - k_1}}{2\sqrt{z^2(\beta^2 k_3 + k_4)}}\right)\right)\right)^2} - \beta^2 + k_1\right)}{2k_2}, \tag{3.40}$$

where

$$A_{29} = h_1\exp\left(z\left(g_2 + \frac{\varrho\sqrt{\beta^2 - k_1}}{2\sqrt{z^2(\beta^2 k_3 + k_4)}}\right)\right) + h_4\cosh\left(z\left(g_6 + \frac{\varrho\sqrt{\beta^2 - k_1}}{2\sqrt{z^2(\beta^2 k_3 + k_4)}}\right)\right), \tag{3.41}$$

$$A_{30} = h_3\sin\left(z\left(g_4 - \frac{\varrho\sqrt{k_1 - \beta^2}}{2\sqrt{z^2(\beta^2 k_3 + k_4)}}\right)\right) + h_4\sinh\left(z\left(g_6 + \frac{\varrho\sqrt{\beta^2 - k_1}}{2\sqrt{z^2(\beta^2 k_3 + k_4)}}\right)\right). \tag{3.42}$$

4 Discussion

In this section, the traveling-wave solutions for the DDE are shown graphically. The purpose is to illustrate the soliton and solitary wave solutions obtained in the previous section. The figures show a variety of soliton solutions in three dimensions along with their matching contours and

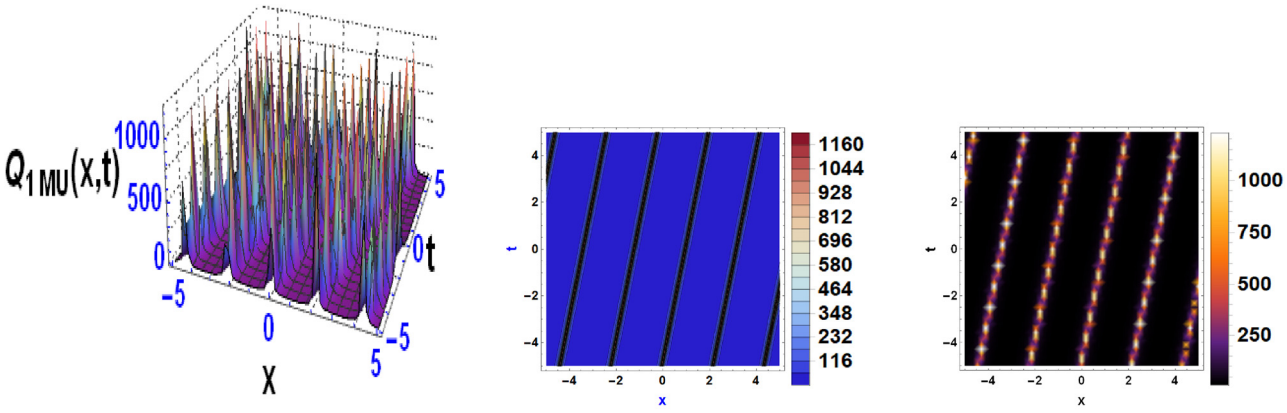

Figure 1: Graphs showing (a) three-dimensional, (b) contour, and (c) density plots of the solution $Q_{1MU}(x, t)$. The graphs were obtained by selecting parameter values $g_2 = 9.7$, $g_4 = 8.7$, $g_6 = 2.9$, $h_1 = 0.6$, $h_2 = 5.3$, $h_3 = 2.9$, $z = 0.04$, $k_1 = 2.09$, $k_2 = 0.6$, $k_3 = 1.2$, $k_4 = 0.2$, and $\beta = 0.2$.

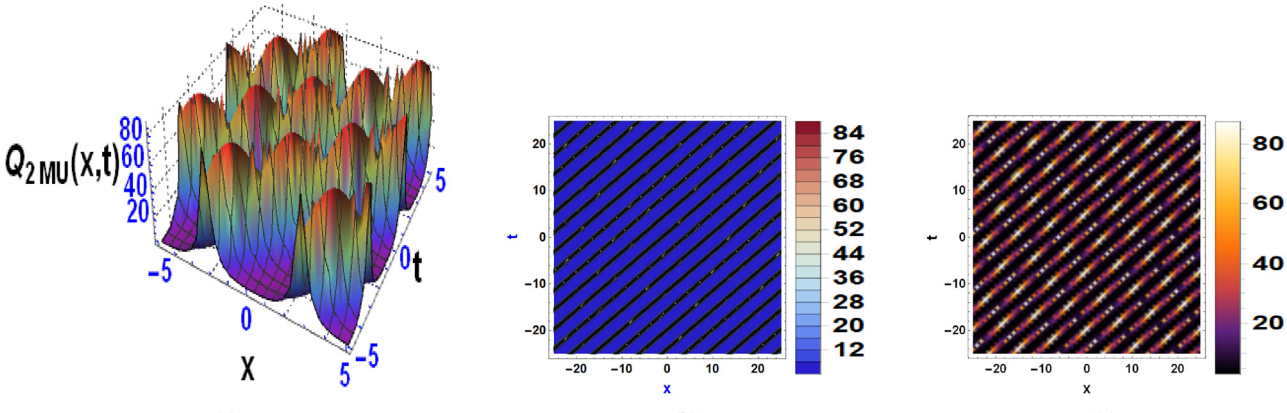

Figure 2: Graphs showing (a) three-dimensional, (b) contour, and (c) density plots of the solution $Q_{2MU}(x, t)$. The graphs were obtained by selecting parameter values $g_4 = 7.2$, $g_6 = 0.3$, $h_2 = 1.7$, $h_3 = 2.3$, $z = 0.38$, $k_1 = 9.4$, $k_2 = 3.7$, $k_3 = 2.3$, $k_4 = 1.7$, and $\beta = 1.2$.

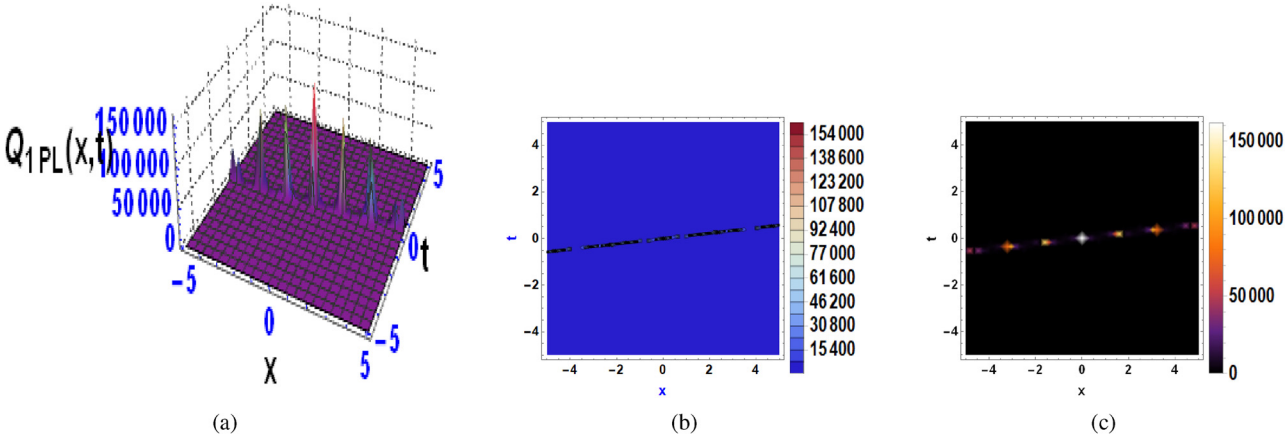

Figure 3: Graphs showing (a) three-dimensional, (b) contour, and (c) density plots of the solution $Q_{1LP}(x, t)$. The chosen parameter values are as follows: $g_6 = 1.549$, $k_1 = 2.23$, $k_2 = 1.43$, $k_3 = 5.28$, $k_4 = 0.3$, and $\beta = 8.7$.

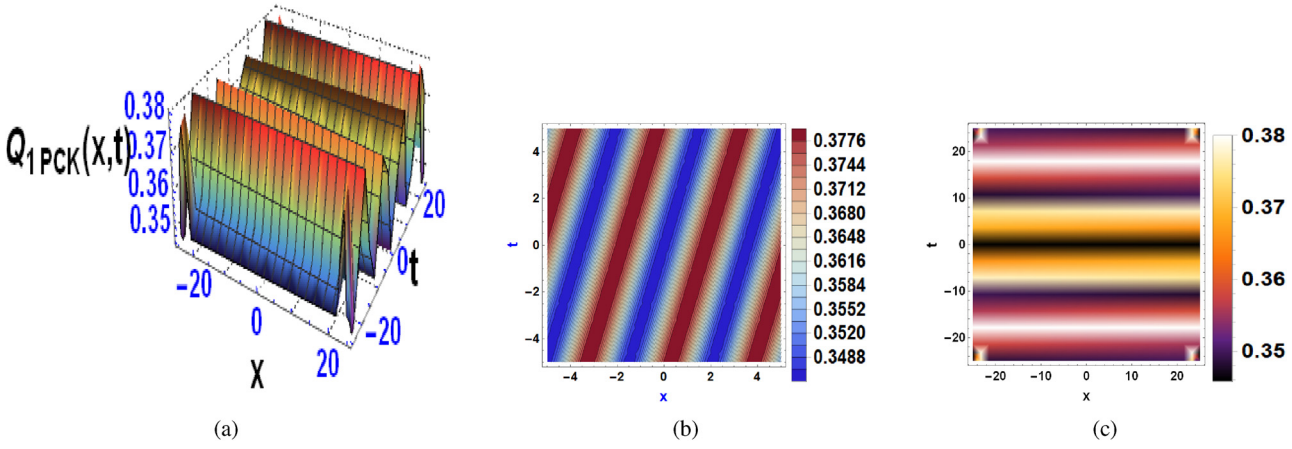

(a) (b) (c)

Figure 4: Graphs showing (a) three-dimensional, (b) contour, and (c) density plots of the solution $Q_{1PCK}(x, t)$ corresponding to the parameter values $g_2 = 8.2$, $g_4 = 2.9$, $g_8 = 2.1$, $h_1 = 6.3$, $h_3 = 8.01$, $z = 4.1$, $k_1 = 5.9$, $k_2 = 2.3$, $k_3 = 3.0$, $k_4 = 1.6$, and $\beta = 0.3$.

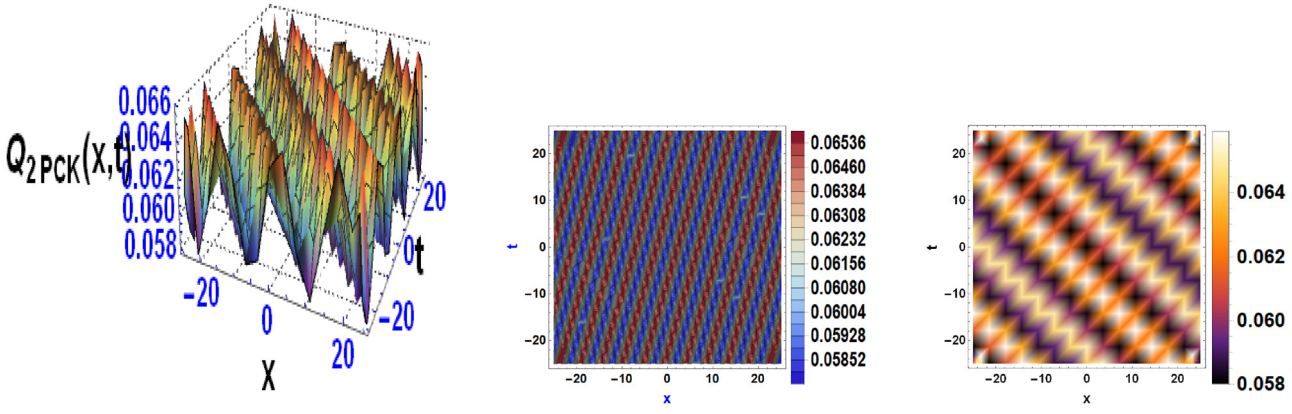

(a) (b) (c)

Figure 5: Graphs showing (a) three-dimensional, (b) contour, and (c) density plots of the solution $Q_{2PCK}(x, t)$ corresponding to the parameter values $g_2 = 1.1$, $g_6 = 4.4$, $g_8 = 2.8$, $h_2 = 4.4$, $h_3 = 2.9$, $k_1 = 1.2$, $z = 1.4$, $k_2 = 3.5$, $k_3 = 1.1$, $k_4 = 0.5$, and $\beta = 0.3$.

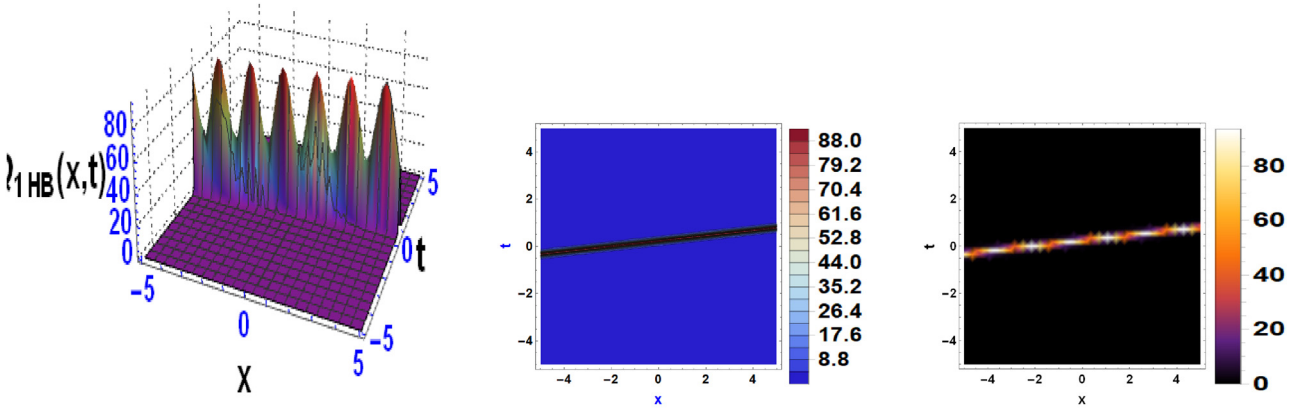

(a) (b) (c)

Figure 6: Graphs showing (a) three-dimensional, (b) contour, and (c) density plots of the solution $Q_{1HB}(x, t)$ corresponding to the parameter values $g_2 = 0.6$, $g_4 = 0.7$, $g_6 = 0.2$, $h_1 = 2.3$, $h_2 = 3.4$, $z = 6.2$, $k_1 = 4.65$, $k_2 = 1.8$, $k_3 = 0.19$, $k_4 = 0.2$, and $\beta = 8.9$.

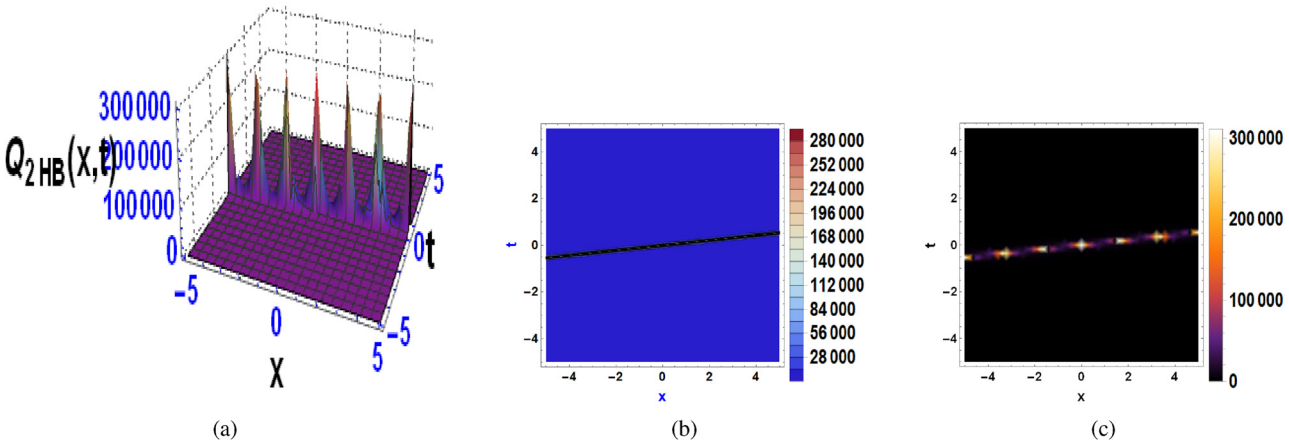

(a) (b) (c)

Figure 7: Graphs showing (a) three-dimensional, (b) contour, and (c) density plots of the solution $Q_{2HB}(x, t)$. The following parameter values were chosen: $g_2 = 8.0$, $g_6 = 9.4$, $h_2 = 3.4$, $z = 1.5$, $k_1 = 0.57$, $k_2 = 0.3$, $k_3 = 9.7$, $k_4 = 1.1$, and $\beta = 9.3$.

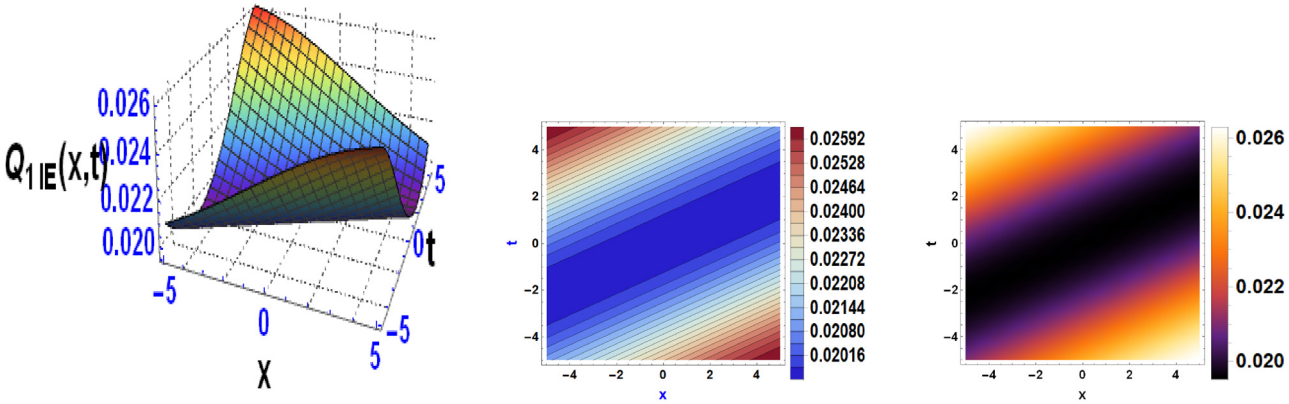

(a) (b) (c)

Figure 8: Graphs showing (a) three-dimensional, (b) contour, and (c) density plots of the solution $Q_{2HB}(x, t)$ for the following choice of parameter values: $g_2 = 0.9$, $g_3 = 3.1$, $g_4 = 2.2$, $h_1 = 8.1$, $h_2 = 2.9$, $z = 1.2$, $k_1 = 4.91$, $k_2 = 1.4$, $k_3 = 0.33$, $k_4 = 0.5$, and $\beta = 2.2$.

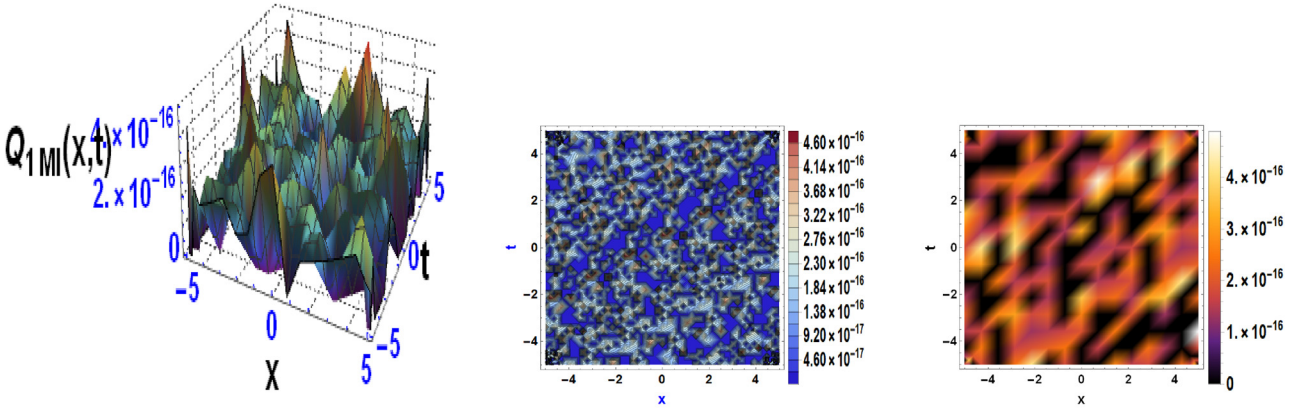

(a) (b) (c)

Figure 9: Graphs showing (a) three-dimensional, (b) contour, and (c) density plots of the solution $Q_{1MI}(x, t)$ corresponding to the parameter values $g_2 = 8.9$, $g_4 = 3.8$, $g_6 = 4.2$, $h_1 = 1.3$, $h_2 = 8.1$, $h_3 = 5.4$, $h_4 = 7.2$, $z = 9.7$, $k_1 = 2.1$, $k_2 = 1.5$, $k_3 = 1.4$, $k_4 = 2.9$, and $\beta = 1.8$.

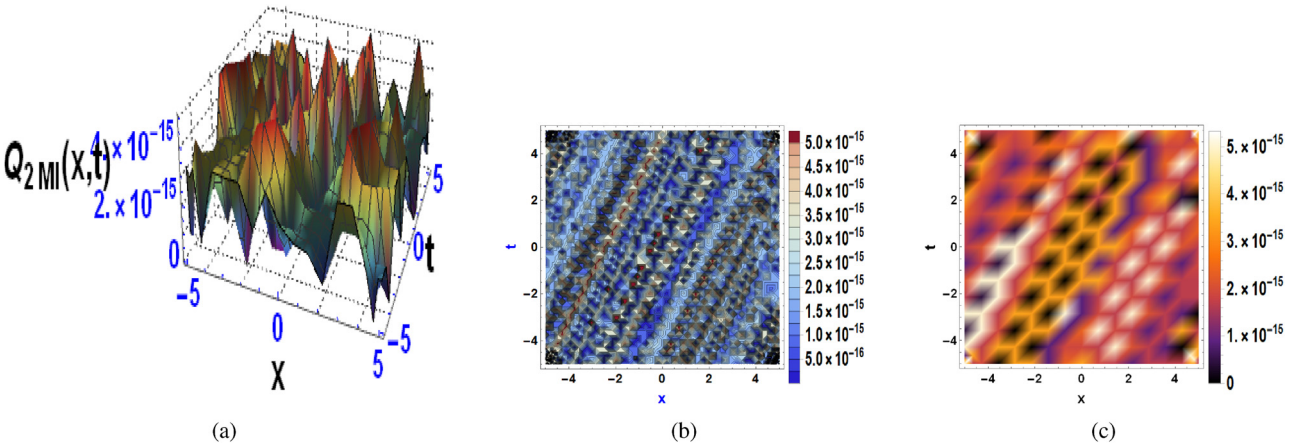

Figure 10: Graphs showing (a) three-dimensional, (b) contour, and (c) density plots of the solution $Q_{2MI}(x, t)$ corresponding to the parameter values $g_2 = 4.7$, $g_4 = 0.2$, $g_6 = 8.7$, $h_1 = 1.1$, $h_3 = 0.1$, $h_4 = 0.1$, $z = 6.1$, $k_1 = 2.13$, $k_2 = 0.2$, $k_3 = 0.6$, $k_4 = 10.0$, and $\beta = 0.5$.

density plots. These solutions include multi-wave, periodic lumps, periodic cross-kink waves, homoclinic breather waves, interaction *via* two-exponent wave structure, and mixed waves. Each of the figures shows (a) 3D graphs, (b) contour plots, and (c) density plots, and details on the functions and parameters used are presented in the caption of each figure. To start with, Figure 1 shows multiple lump-type waves arising from the multi-wave structure function, while Figure 2 depicts multiple breather waves arising from the multi-wave structure function. In turn, Figure 3 shows periodic bright lump waves derived from the periodic lump wave profile function. Figures 4 and 5 show periodic cross-kink wave profiles. Figures 6 and 7 show bright breather waves obtained from the homoclinic breather wave function. Figure 8 shows a dark soliton derived from the structure function of interaction between double exponents. Finally, Figures 9 and 10 show mixtures of wave shapes in the form of solitary waves, derived from the mixed wave function. Multiple wave solutions, periodic lump waves, and mixed waves are all different physical behaviors in nonlinear systems. Multiple wave solutions involve the collision of several solitary waves, *e.g.*, solitons, that keep their shape and speed even after collision. Periodic lump waves are localized waves that appear periodically in space or time, having lump-like features with a periodic structure. Mixed waves are the coexistence or interaction of multiple wave types such as a soliton on a periodic wave leading to hybrid, complex dynamics. They occur in many physical situations across fluid mechanics, optics, and plasma physics, where nonlinear wave–wave interactions control wave development.

It is worth noting that multi-wave solutions depict how several interacting primary wave fronts of diverse contents lead to the emergence of distortion and stress profiles. Periodic lump waves illustrate how energy is being sustained within given intervals, thereby showing that the material is subjected to compressive forces for a while before being released. These wave types are crucial in elucidating the ability of elastic rods to store and transmit energy in a cyclical manner, which is a key aspect in the study of wave motion in solids. Furthermore, periodic cross-kink waves show clear uniform regions that are interleaved with narrower regions of apparent distortion, which may suggest buckling or sudden high straining rates in elastic materials under load. Also, we observe that homoclinic breather waves can persist where the oscillations are confined, suggesting that sufficiently long waves with little energy leakage from the rod can be sustained. These aspects help explain the non-trivial content of nonlinear wave propagation in elastic solids. Dark solitons and mixed wave solutions show that there are many ways in which waves interact in Murnaghan's rods. In this case, dark solitons are areas of depressions or less deformed medium showing some stabilization of the material, whereas mixed wave solutions showcase the fact that elastic rods are capable of having even simultaneous different types of wave motion propagating within them. These facts highlight the intricacy of wave motions in elastic structures and may prove useful for engineering designs as well as for nonlinear wave propagation research in solids.

The physical interpretation of the model parameters helps improve the practical insight into the wave structures obtained. In particular, the parameter β signifies the velocity of the wave and the speed with which disturbances travel within the elastic Murnaghan's rod. The amplitude of the solutions, as it is dependent on parameters such as m, h_1, h_2, and h_3, reflects the intensity of strain or deformation the medium undergoes. Material-

dependent constants k_1, k_2, k_3, and k_4 control the relative strength of dispersion and nonlinearity, determining the temporal evolution of wave profiles. Additionally, the spatial localization of derived solutions, for example, lump and breather waves, indicates that energy is localized in space, and thus, these waveforms are highly applicable for NDT and energy-guided transmission in elastic media.

The values utilized in the graphical plots were arbitrarily chosen to ensure visibility, clarity, and variability of the wave structures in question. The values are not experimentally obtained but were selected within physically reasonable ranges to characterize the qualitative character of the exact solutions. The main aim was to exhibit richness of solution space and the effect of parameter variation on wave shape, localization, and interaction. Additional work can include tuning these parameters against actual material properties for application-oriented modeling.

5 Comparison

The solutions achieved in this work, obtained through the Hirota bilinear method, are a major improvement over most of the earlier reported outcomes for DDE as in nonlinear elastic rods. Previous studies have used a wide range of analytical methods such as the sine-Gordon expansion technique [34], extended sinh-Gordon and modified $\exp(-\phi(\xi))$ techniques [27], enhanced modified extended tanh-function method [35], generalized exponential rational and Jacobi elliptic function methods [36], and SSEMs [37,39], for obtaining exact solutions. The studies yielded various soliton and periodic waveforms such as bright and dark solitons, kink and anti-kink waves, hyperbolic, trigonometric, and elliptic solutions. Although such methods are successful, they tend to produce isolated wave structures and may be restrictive in fully capturing the entire richness of nonlinear wave behavior in elastic media.

In contrast, the Hirota bilinear approach is a better structured and integrated procedure that can build up diverse and composite wave structures, including multi-wave interaction, periodic lumps, cross-kink waves, homoclinic breathers, and mixed solitons. The variety of solution types reflects a better insight into the nonlinear processes that govern wave propagation in elastic rods such as those accommodated by Murnaghan's theory. The capacity of this method to generate topological and non-topological, localized and periodic, and bright and dark soliton solutions places it well in comparison to other analytical methods. In contrast to recent researches involving coupled nonlinear Schrödinger equations that also utilize the Hirota technique to discover new optical soliton structures [48], the present contribution expands its application to mechanical wave systems and thus presents a broader understanding of intricate wave phenomenon in doubly dispersive and nonlinear elastic systems.

6 Conclusion

In this work, we used the Hirota bilinear transformation approach to derive various wave structures, which are solutions of a DDE in an elastic Murnaghan's rod. Using the Hirota technique, we were able to obtain traveling-wave solutions in the form of periodic lump waves, periodic cross-kink waves, homoclinic breather waves, dark soliton, and mixed waves. In addition, the complex structures and interactions of these wave structures were illustrated in the form of 3D, contour, and density plots. The graphical representations illustrate that the shape of the wave affects the propagation of the wave itself. This is particularly evident in the density plots and wave interaction patterns. As a comment, this method has the ability to describe the deformation of single solitary waves in an elastic perfect material and can suggest how such systems behave physically. To the best of our knowledge, this is the first study in which the Hirota bilinear method is used in the context of doubly dispersive media, and the results derived in this manuscript may apply to both fundamental and practical investigations, especially for engineering designs involving elastic wave propagation.

Future work might involve the examination of the stability, chaos, and perturbation response of the DDE to determine its robustness in the presence of small disturbances. The inclusion of fractional-order derivatives would enable the modeling of memory and hereditary effects in viscoelastic or incompressible elastic materials. Adding stochastic terms could potentially facilitate the inclusion of uncertainties and random disturbance that are generally found in real environments. The other possibility is the generalization of the model to a variable-coefficient problem, which would be more representative of spatial or temporal inhomogeneities of the material. These developments would not only improve theoretical insight into the DDE but also extend its availability to a wider range of physical systems, such as composite materials, biological tissue, and engineered smart materials.

Acknowledgments: The authors wish to thank the anonymous reviewers for their comments. All of their criticisms and suggestions were followed *at litteram*, resulting in a substantial improvement on the overall quality of this work.

Funding information: The authors state no funding involved.

Author contributions: Conceptualization, N.A., and J.E.M.D.; methodology, N.A., and; software, B.C., S.M., M.Z.B., N.A., A.R.-L., and J.E.M.-D.; validation, B.C., S.M., M.Z.B., N.A., A.R.-L., and J.E.M.-D.; formal analysis, B.C., S.M., M.Z.B., N.A., and J.E.M.-D.; investigation, N.A., and J.E.M.-D.; resources, B.C., S.M., M.Z.B., N.A., A.R.-L., and J.E.M.-D.; data curation, B.C., S.M., M.Z.B., N.A., A.R.-L., and J.E.M.-D.; writing – original draft preparation, B.C., S.M., M.Z.B., N.A., A.R.-L., and J.E.M.-D.; writing – review and editing, B.C., S.M., M.Z.B., N.A., A.R.-L., and J.E.M.-D.; visualization, B.C.; supervision, N.A., and J.E.M.-D. All authors have accepted responsibility for the entire content of this manuscript and approved its submission.

Conflict of interest: Jorge E. Macías-Díaz, who is the co-author of this article, is a current Editorial Board member of *Open Physics*. This fact did not affect the peer-review process. The authors state no other conflict of interest.

Data availability statement: The datasets generated and/or analysed during the current study are available from the corresponding author on reasonable request.

References

[1] Kumar M Exact solutions of systems of nonlinear time-space fractional partial differential equations using an iterative method. J Comput Nonlinear Dyn. 2023;18(10):101003.

[2] Dubey VP, Singh J, Alshehri AM, Dubey S, Kumar D. Analysis and fractal dynamics of local fractional partial differential equations occurring in physical sciences. J Comput Nonlinear Dyn. 2023;18(3):031001.

[3] Baber MZ, Yasin MW, Xu C, Ahmed N, Iqbal MS. Numerical and analytical study for the stochastic spatial dependent prey-predator dynamical system. J Comput Nonlinear Dyn. 2024;19:10.

[4] Akbulut A, Islam SR. Study on the Biswas-Arshed equation with the beta time derivative. Int J Appl Comput Math. 2022;8(4):167.

[5] Alharbi AR, Almatrafi MB, Lotfy K. Constructions of solitary travelling wave solutions for Ito integro-differential equation arising in plasma physics. Results Phys. 2020;19:103533.

[6] Agrawal GP. Nonlinear fiber optics. In: Nonlinear Science at the Dawn of the 21st Century. Berlin, Heidelberg: Springer Berlin Heidelberg; 2000. pp. 195–211.

[7] Ceesay B, Ahmed N, Baber MZ, Akgul A. Breather, lump, M-shape and other interaction for the Poisson-Nernst-Planck equation in biological membranes. Opt Quantum Electron. 2024;56(5):853.

[8] Wang P, Yin F, urRahman M, Khan MA, Baleanu D. Unveiling complexity: Exploring chaos and solitons in modified nonlinear Schrödinger equation. Results Phys. 2024;56:107268.

[9] Zahed H, Seadawy AR, Iqbal M. Structure of analytical ion-acoustic solitary wave solutions for the dynamical system of nonlinear wave propagation. Open Phys. 2022;20(1):313–33.

[10] Peng X, Zhao YW, Lu X. Data-driven solitons and parameter discovery to the (2+1)-dimensional NLSE in optical fiber communications. Nonlinear Dyn. 2024;112(2):1291–306.

[11] Barsoum MW, Murugaiah A, Kalidindi SR, Zhen T. Kinking nonlinear elastic solids, nanoindentations, and geology. Phys Rev Lett. 2004;92(25):255508.

[12] Thomas BB, Betchewe G, Victor KK, Crepin KT. On periodic wave solutions to (1+1)-dimensional nonlinear physical models using the Sine-Cosine method. Acta Appl Math. 2010;110:945–53.

[13] Nofal TA. Simple equation method for nonlinear partial differential equations and its applications. J Egypt Math Soc. 2016;24(2):204–9.

[14] Hussain S, Iqbal MS, Ashraf R, Inc M, Tarar MA. Exploring nonlinear dispersive waves in a disordered medium: an analysis using ϕ^6 model expansion method. Opt Quantum Electron. 2023;55(7):651.

[15] Baber MZ, Seadway AR, Iqbal MS, Ahmed N, Yasin MW, Ahmed MO. Comparative analysis of numerical and newly constructed soliton solutions of stochastic Fisher-type equations in a sufficiently long habitat. Int J Modern Phys B. 2023;37(16):2350155.

[16] Lu X, Chen SJ. Interaction solutions to nonlinear partial differential equations via Hirota bilinear forms: one-lump-multi-stripe and one-lump-multi-soliton types. Nonlinear Dyn. 2021;103(1):947–77.

[17] Khan MI, Farooq A, Nisar KS, Shah NA. Unveiling new exact solutions of the unstable nonlinear Schrödinger equation using the improved modified Sardar sub-equation method. Results Phys. 2024;59:107593.

[18] Baber MZ, Abbas G, Saeed I, Sulaiman TA, Ahmed N, Ahmad H, et al. Optical solitons for 2D-NLSE in multimode fiber with Kerr nonlinearity and its modulation instability. Modern Phys Lett B. 2024;2450341.

[19] Wei L. A function transformation method and exact solutions to a generalized sinh-Gordon equation. Comput Math Appl. 2010;60(11):3003–11.

[20] Batool F, Rezazadeh H, Ali Z, Demirbilek U. Exploring soliton solutions of stochastic Phi-4 equation through extended Sinh-Gordon expansion method. Opt Quantum Electron. 2024;56(5):785.

[21] Kadkhoda N Application of $\frac{G'}{G^2}$-expansion method for solving fractional differential equations. Int J Appl Comput Math. 2017;3:1415–24.

[22] Ali A, Ahmad J, Javed S. Dynamic investigation to the generalized Yu-Toda-Sasa-Fukuyama equation using Darboux transformation. Opt Quantum Electron. 2024;56(2):166.

[23] Abdel-Gawad H. I. Field and reverse field solitons in wave-operator nonlinear Schrödinger equation with space-time reverse: Modulation instability. Commun Theoret Phys. 2023;75(6):065005.

[24] Hosseini K, Alizadeh F, Hinçal E, Ilie M, Osman MS. Bilinear Bäcklund transformation, Lax pair, Painlevé integrability, and different wave structures of a 3D generalized KdV equation. Nonlinear Dyn. 2024;112(20):18397–411.

[25] Kumar M, Jhinga A, Majithia JT. Solutions of time-space fractional partial differential equations using Picard's iterative method. J Comput Nonlinear Dyn. 2024;19(3):031006.

[26] Fafa W, Odibat Z, Shawagfeh N. The homotopy analysis method for solving differential equations With generalized Caputo-type fractional derivatives. J Comput Nonlinear Dyn 2023;18(2):021004.

[27] Cattani C, Sulaiman TA, Baskonus HM, Bulut H. Solitons in an inhomogeneous Murnaghan's rod. Europ Phys J Plus. 2018;133:1–11.

[28] Samsonov AM. Strain solitons in solids and how to construct them. CRC Press; 2001.

[29] Rushchitsky JJ, Cattani C. Similarities and differences between the Murnaghan and Signorini descriptions of the evolution of quadratically nonlinear hyperelastic plane waves. Int Appl Mech. 2006;42:997–1010.

[30] Silambarasan R, Baskonus HM, Bulut H. Jacobi elliptic function solutions of the double dispersive equation in the Murnaghan's rod. Europ Phys J Plus. 2019;134:1–22.

[31] Rani M, Ahmed N, Dragomir SS, Mohyud-Din ST, Khan I, Nisar KS. Some newly explored exact solitary wave solutions to nonlinear

inhomogeneous Murnaghan's rod equation of fractional order. J Taibah Univ Sci. 2021;15(1):97–110.
[32] Dusunceli F, Celik E, Askin M, Bulut H. New exact solutions for the doubly dispersive equation using the improved Bernoulli sub-equation function method. Indian J Phys. 2021;95:309–14.
[33] Alquran M, Al Smadi T Generating new symmetric bi-peakon and singular bi-periodic profile solutions to the generalized doubly dispersive equation. Opt Quantum Electron. 2023;55(8):736.
[34] Yel G. New wave patterns to the doubly dispersive equation in nonlinear dynamic elasticity. Pramana. 2020;94(1):79.
[35] Ahmed MS, Zaghrout AA, Ahmed HM. Travelling wave solutions for the doubly dispersive equation using improved modified extended tanh-function method. Alexandr Eng J. 2022;61(10):7987–94.
[36] Alharthi M. S. Wave solitons to a nonlinear doubly dispersive equation in describing the nonlinear wave propagation via two analytical techniques. Results Phys. 2023;47:106362.
[37] Rehman SU, Seadawy AR, Rizvi STR, Ahmed S, Althobaiti S. Investigation of double dispersive waves in nonlinear elastic inhomogeneous Murnaghan's rod. Modern Phys Lett B. 2022;36(8):2150628.
[38] Ozisik M, Secer A, Bayram M, Sulaiman TA, Yusuf A Acquiring the solitons of inhomogeneous Murnaghan's rod using extended Kudryashov method with Bernoulli–Riccati approach. Int J Modern Phys B. 2022;36(30):2250221.
[39] Ibrahim S, Sulaiman TA, Yusuf A, Ozsahin DU, Baleanu D. Wave propagation to the doubly dispersive equation and the improved Boussinesq equation. Opt Quantum Electron. 2024;56(1):20.
[40] Younas U, Bilal M, Sulaiman TA, Ren J, Yusuf A. On the exact soliton solutions and different wave structures to the double dispersive equation. Opt Quantum Electron. 2022;54:1–22.
[41] Abourabia AM, Eldreeny YA. A soliton solution of the DD-equation of the Murnaghan's rod via the commutative hyper complex analysis. Partial Differ Equ Appl Math. 2022;6:100420.
[42] Asjad MI, Faridi WA, Jhangeer A, Ahmad H, Abdel-Khalek S, Alshehri N. Propagation of some new traveling wave patterns of the double dispersive equation. Open Phys. 2022;20(1):130–41.
[43] Dusunceli F, Celik E, Askin M, Bulut H New exact solutions for the doubly dispersive equation using the improved Bernoulli sub-equation function method. Indian J Phys. 2021;95:309–14.
[44] Eremeyev VE, Kolpakov AG. Solitary waves in Murnaghan's rod: Numerical simulations based on the generalized dispersive model. J Appl Mech Tech Phys. 2012;53(4):565–75.
[45] Eremeyev VE, Movchan AB Movchan NV. Dispersion properties of harmonic waves in a rod with a nonuniform cross section. J Eng Math. 2016;98(1):1–18.
[46] Islam SR Bifurcation analysis and soliton solutions to the doubly dispersive equation in elastic inhomogeneous Murnaghan's rod. Sci Rep. 2024;14(1):11428.
[47] Khatun MM, Gepreel KA, Akbar MA. Dynamics of solitons of the ß-fractional doubly dispersive model: stability and phase portrait analysis. Indian J Phys. 2025;1–16. doi: 10.1007/s12648-025-03602-3.
[48] Khater M, Wang H, Alfalqi SH, Vokhmintsev A, Owyed S. Insights into acoustic beams in nonlinear, weakly dispersive and dissipative media. Opt Quantum Electron. 2025;57(5):1–18.
[49] Naz S, Rani A, Ul Hassan QM, Ahmad J, Rehman SU, Shakeel M. Dynamic study of new soliton solutions of time-fractional longitudinal wave equation using an analytical approach. Int J Modern Phys B. 2024;38(31):2450420.
[50] Alsallami SA, Rizvi ST, Seadawy AR. Study of stochastic-fractional Drinfelad-Sokolov-Wilson equation for M-shaped rational, homoclinic breather, periodic and Kink-Cross rational solutions. Mathematics. 2023;11(6):1504.
[51] Garcia Guirao JL, Baskonus HM, Kumar A. Regarding new wave patterns of the newly extended nonlinear (2+1)-dimensional Boussinesq equation with fourth order. Mathematics. 2020;8(3):341.
[52] Ceesay B, Baber MZ, Ahmed N, Akguuul A, Cordero A, Torregrosa JR. Modelling symmetric ion-acoustic wave structures for the BBMPB equation in fluid ions using Hirotaas bilinear technique. Symmetry 2023;15(9):1682.
[53] Yang XF, Wei Y Bilinear equation of the nonlinear partial differential equation and its application. J Funct Spaces 2020;2020(1)4912159.
[54] Wazwaz AM. The Hirota's direct method and the tanh–coth method for multiple-soliton solutions of the Sawada-Kotera-Ito seventh-order equation. Appl Math Comput. 2008;199(1):133–8.
[55] Hereman W, Zhuang W. Symbolic computation of solitons via Hirota's bilinear method. Department of Mathematical and Computer Sciences, Colorado, School of Mines. 1994.
[56] Rizvi ST, Seadawy AR, Nimra, Ahmad A. Study of lump, rogue, multi, M shaped, periodic cross kink, breather lump, kink-cross rational waves and other interactions to the Kraenkel-Manna-Merle system in a saturated ferromagnetic material. Opt Quantum Electron. 2023;55(9):813.
[57] Wang M, Tian B, Quuu QX, Zhao XH, Zhang Z, Tian HY. Lump, lumpoff, rogue wave, breather wave and periodic lump solutions for a (3+1)-dimensional generalized Kadomtsev-Petviashvili equation in fluid mechanics and plasma physics. Int J Comput Math. 2020;97(12):2474–86.
[58] Khan MH, Wazwaz AM. Lump, multi-lump, cross kinky-lump and manifold periodic-soliton solutions for the (2+1)-D Calogero-Bogoyavlenskii-Schiff equation. Heliyon. 2020;6(4):e03701.
[59] Zhao Z, Chen Y, Han B. Lump soliton, mixed lump stripe and periodic lump solutions of a (2+1)-dimensional asymmetrical Nizhnik-Novikov-Veselov equation. Modern Phys Lett B. 2017;31(14):1750157.
[60] Ren B, Lin J, Lou ZM. A new nonlinear equation with lump-soliton, lump-periodic, and lump-periodic-soliton solutions. Complexity. 2019;2019(1):4072754.
[61] Rizvi STR, Seadawy AR, Ashraf MA, Bashir A, Younis M, Baleanu D. Multi-wave, homoclinic breather, M-shaped rational and other solitary wave solutions for coupled-Higgs equation. Europ Phys J Special Topics. 2021;230(18):3519–32.
[62] Yel G, Cattani C, Baskonus HM, Gao W. On the complex simulations with dark-bright to the Hirota-Maccari system. J Comput Nonlinear Dyn. 2021;16(6):061005.
[63] Ozsahin DU, Ceesay B, Baber MZ, Ahmed N, Raza A, Rafiq M, et al. Multiwaves, breathers, lump and other solutions for the Heimburg model in biomembranes and nerves. Sci Rep. 2024;14(1):10180.
[64] Ceesay B, Ahmed N, Macías-Díaz JE. Construction of M-shaped solitons for a modified regularized long-wave equation via Hirota's bilinear method. Open Phys. 2024;22(1):20240057.
[65] Tedjani AH, Seadawy AR, Rizvi ST, Solouma E. Dynamical structure and soliton solutions galore: investigating the range of forms in the perturbed nonlinear Schrödinger dynamical equation. Opt Quantum Electron. 2024;56(5):764.
[66] Ceesay B, Baber MZ, Ahmed N, Macías S, Macías-Díaz JE, Medina-Guevara MG. Solitonic wave solutions of a Hamiltonian nonlinear atom chain model through the Hirota bilinear transformation method. Open Phys. 2025;23(1):20250150.
[67] Rizvi ST, Seadawy AR, Ahmed S. Bell and Kink type, Weierstrass and Jacobi elliptic, multiwave, kinky breather, M-shaped and periodic-kink-cross rational solutions for Einstein's vacuum field model. Opt Quantum Electron. 2024;56(3):456.